

AD-A031 439

ARMY ELECTRONICS COMMAND FORT MONMOUTH N J
AN ALL DIGITAL AUTOMATED WIND MEASUREMENT SYSTEM.(U)
SEP 76 F TAYLOR , P MOHAN, P JOSEPH, T PRIES

F/G 4/2

UNCLASSIFIED

ECOM-5801

NL

1 OF 1
AD
A031439





AD A 031 439

AD

Reports Control Symbol
OSD-1366

12

RESEARCH AND DEVELOPMENT TECHNICAL REPORT
ECOM-5801

AN ALL DIGITAL AUTOMATED WIND MEASUREMENT SYSTEM

By

F. Taylor
P. Mohan
University of Cincinnati

P. Joseph
Globe Universal Sciences
El Paso, Texas

and

T. Pries

Atmospheric Sciences Laboratory

US Army Electronics Command
White Sands Missile Range, New Mexico 88002

September 1976

Approved for public release; distribution unlimited.

DDC
RECEIVED
NOV 1 1976
A

ECOM

UNITED STATES ARMY ELECTRONICS COMMAND - FORT MONMOUTH, NEW JERSEY 07703

NOTICES

Disclaimers

The findings in this report are not to be construed as an official Department of the Army position, unless so designated by other authorized documents.

The citation of trade names and names of manufacturers in this report is not to be construed as official Government indorsement or approval of commercial products or services referenced herein.

Disposition

Destory this report when it is no longer needed. Do not return it to the originator.

REPORT DOCUMENTATION PAGE		READ INSTRUCTIONS BEFORE COMPLETING FORM
1. REPORT NUMBER 14 ECOM-5801	2. GOVT ACCESSION NO.	3. RECIPIENT'S CATALOG NUMBER
4. TITLE (and Subtitle) AN ALL DIGITAL AUTOMATED WIND MEASUREMENT SYSTEM	5. TYPE OF REPORT & PERIOD COVERED Research and development technical rept.	
7. AUTHOR(s) 10 F. Taylor, P. Mohan, P. Joseph, and T. Pries	6. PERFORMING ORG. REPORT NUMBER	
9. PERFORMING ORGANIZATION NAME AND ADDRESS Atmospheric Sciences Laboratory White Sands Missile Range, New Mexico 88002	8. CONTRACT OR GRANT NUMBER(s)	
11. CONTROLLING OFFICE NAME AND ADDRESS US Army Electronics Command Fort Monmouth, New Jersey 07703	10. PROGRAM ELEMENT, PROJECT, TASK AREA & WORK UNIT NUMBERS DA Task No. IST61102B53A SA3	
14. MONITORING AGENCY NAME & ADDRESS (if different from Controlling Office)	12. REPORT DATE 11 September 1976	13. NUMBER OF PAGES 29 (12 top)
	15. SECURITY CLASS. (of this report) UNCLASSIFIED	
16. DISTRIBUTION STATEMENT (of this Report) Approved for public release; distribution unlimited.		
17. DISTRIBUTION STATEMENT (of the abstract entered in Block 20, if different from Report)		
18. SUPPLEMENTARY NOTES		
19. KEY WORDS (Continue on reverse side if necessary and identify by block number) Anemometer Wind Automated system		
20. ABSTRACT (Continue on reverse side if necessary and identify by block number) In addition to supplying basic meteorological information, vectored wind velocity measurements are essential to the analysis of small caliber ballistic trajectories, optical wave propagation in the lower atmosphere, and wind shears and vorticies. Conventional electromechanical methods, using velocity-to-direct current converters, are often unsatisfactory when integrated into a multisensor array over long path lengths. An all digital system capable of		

ABSTRACT (Cont) *RG P1473 A*

operating as an array over long path lengths has been developed. The system is totally automated. By use of complete metal oxidized semiconductors (CMOS) signal processing remote data acquisition stations, operated under microprocessor control, reliable and accurate asynchronous data transfer has been obtained.

*A**1473 B*

PREFACE

The authors express their gratitude to Mr. W. Hatch and Mr. D. Favier, Atmospheric Sciences Laboratory, White Sands Missile Range, New Mexico, for their technical assistance.

ACCESSION NO.	
NTIS	Whole Section <input checked="" type="checkbox"/>
DDC	Diff Section <input type="checkbox"/>
UNANNOUNCED	<input type="checkbox"/>
JUSTIFICATION.....	
BY.....	
DISTRIBUTION/AVAILABILITY CODES	
Dist.	MAIL, BOOK, SPECIAL
A	

CONTENTS

	<u>Page</u>
INTRODUCTION	3
SYSTEM ARCHITECTURE	7
OPERATION	12
RESULTS	12
CONCLUSIONS	18
APPENDIX	19
Ambiguity Resolution Circuit	19

INTRODUCTION

Vectored wind velocity information is needed to accurately quantify high velocity ordnance ballistics, scattering of high energy lasers, optical communication data rates in lower atmospheric scintillation, aircraft vortex motion, and so forth. Due to the physical size of these events, integrated wind measurements over long path lengths must be obtained. Since direct wind metering devices are point measurement systems, they must be used in an array (Fig. 1). To design and operate an arrayed system in a field environment, unique attributes must be engineered into that system. At present, acoustic or propeller driven anemometers are used to measure direct wind. Since acoustic devices are very expensive from a per unit standpoint (\$30,000), they were not considered for use in a multisensor arrayed system. The less expensive propeller driven devices (less than \$1,000 each) were chosen as the principal transducer of the system. With this hardware restriction imposed, the field array system should possess the following qualities:

- Accurate, reliable measurement of wind velocities
- Ability to support a large number of remote units over long path lengths
- Interactive operator control and automated operation
- High dynamic range and the ability to inhibit ambiguous counts*
- Low installation, maintenance, and servicing costs and easy fault analysis
- Low battery power consumption at remote units and minimal line installation and maintenance times
- Ability to function under severe environmental conditions
- Ability to present data in a format suitable for digital analysis
- Ability to maintain calibration in hostile environments

*An ambiguous count is induced by shaft oscillations about a point where the oscillations are erroneously interpreted as complete shaft rotation.

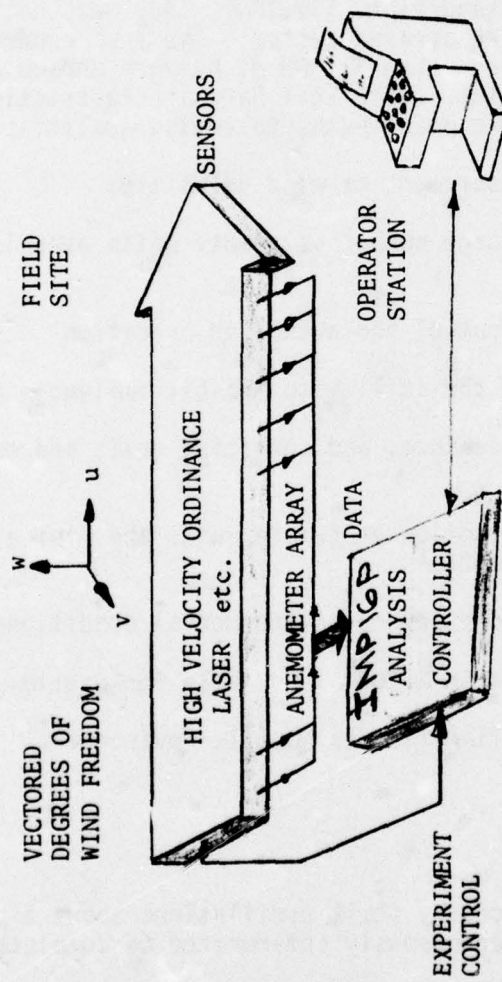


Figure 1. Field operations.

Existing stand-alone propeller driven anemometer systems fall into these two classes:

 Analog: wind speed-to-shaft rotation-to-dc voltage conversion

 Electro-optical: wind speed-to-shaft rotation-to-electronic pulse conversion.

Analog methods, though low power (i.e., a source rather than sink), are prone to lose calibration, become corrupted with analog noise over long transmission paths, and require multi-input summing amplifiers to process arrayed data or an A/D converter if computer analysis is required. Although capable of maintaining calibration and signal integrity over long path lengths, existing transistor to transistor logic (TTL) electro-optical anemometer methods consume too much power for remote field use (i.e., high power digital logic), do not resolve the ambiguity problem, and require custom communication interfacing if asynchronous array data processing is to be allowed. Therefore, existing systems would not satisfy the previously stated design objectives.

The decision was to design an electronic system which would possess as many of the desired attributes as possible. To expedite the design processes, the mechanical housing, bearing assembly, and propeller of an existing analog anemometer were left intact. The dc motor was replaced with an electromechanical system. The output of the anemometer device was a pulse train in one-to-one correspondence with shaft rotations. Calibration was performed in a low-speed wind tunnel or by use of manufacturer's supplied air screw information. Unlike the analog system, which is prone to lose calibration due to amplifier drift and variability in a long low-grade analog communication channel, the digital system will perform accurately over long periods of time; that is, the anemometer will remain calibrated as long as the propeller and bearing assembly remain structurally unchanged. The electronic signal produced by the new transducer was processed by custom-designed low-power CMOS hardware. The entire system was then interfaced to an asynchronous communication line and microprocessor.

The developed system was capable of supporting up to 128 wind monitoring stations (Fig. 2). Each station consists of battery power supply, electronics, and three orthogonal anemometers (denoted U, V, and W directions). Each remote station was connected to an inexpensive low-grade twisted pair of wires. The line drivers used were rated at 1 Mbit/sec at 2.5 km. The system was controlled through the use of a National IMP-16-P microprocessor.

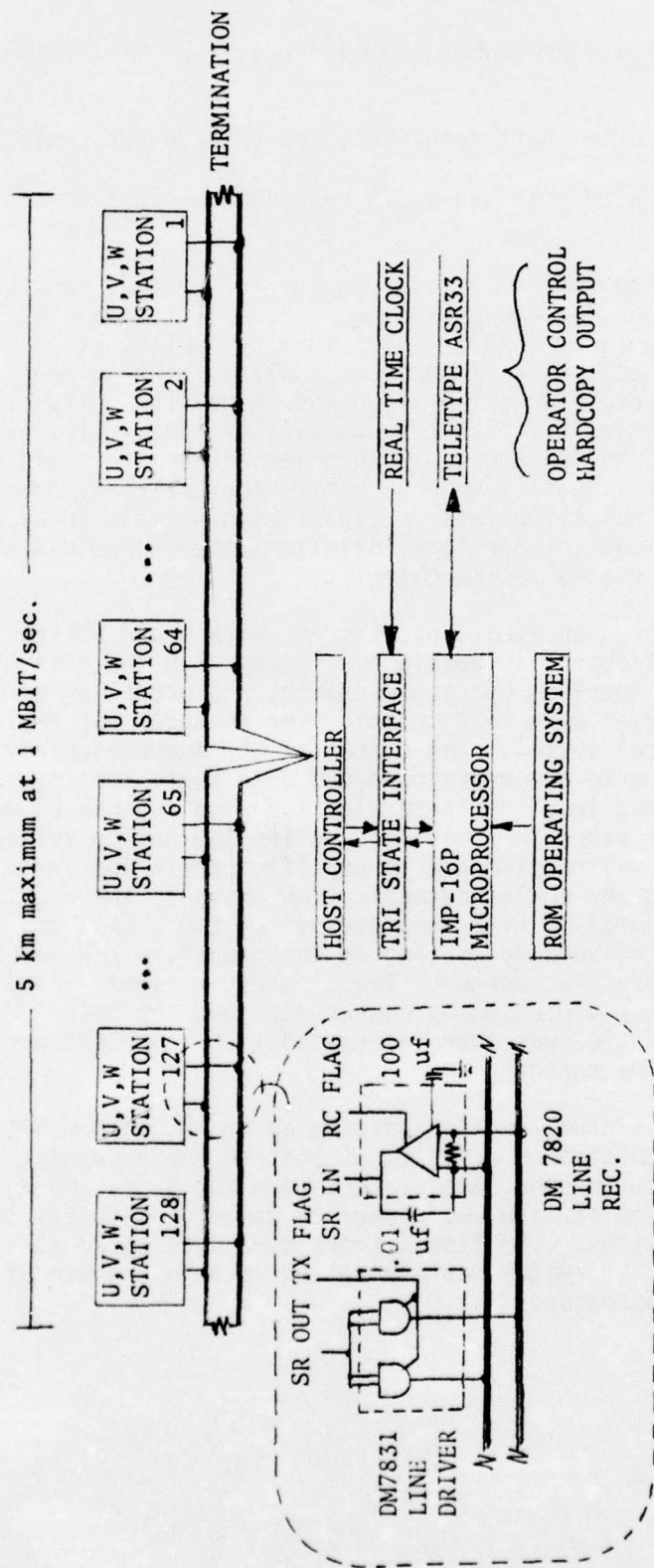


Figure 2. Anemometer array system.

SYSTEM ARCHITECTURE

All point-to-point data and control communication was accomplished through a 20-bit word consisting of 16 bits of information and two start and two stop bits. Conceptually, the developed system functioned as follows:

The pulse train resulting from anemometer shaft rotations, including direction, were shaped, preprocessed (scaled), and presented to an up/down counter.

The up/down counter stored the algebraic count initiated with a system clear-start request. This computer-issued command was received by all remote stations simultaneously.

The remote units were allowed to accumulate data over a user supplied data collection interval. At the end of that interval, a system-wide terminate command was issued to all stations.

The U, V, and W components of any on-line station were then randomly accessed. This initiated a series of events which transferred the appropriate wind component data from the chosen remote station to a custom CMOS asynchronous serial transmitter. The parallel loaded data were then transmitted to the computer for storage and future analysis.

In software, the current and previous counts from a randomly accessed location are differenced. Windspeed can easily be computed from knowledge of the differential count and the averaging interval.

In addition, the current U and V direction counts are compared against 4000_{16} . As long as the U and V counts are below this value, their 16-bit accumulators are assumed to be safe from overflowing during the next averaging interval. If all randomly accessed U and V components pass this test, no system-wide clear command is issued at the end of the data acquisition sequence. The inhibiting of the clear command releases more system time for actual data collecting. If the test fails, a system-wide clear command is issued and counting resumes from zero. Since the 12-bit W component accumulates only extremely low velocity vertical wind information, no overflow sensing software test is provided in this direction.

Figure 3 shows the mechanization of this design philosophy. Certain hardware features of the system, whose implementation is unique to the system developed, will now be investigated in detail.

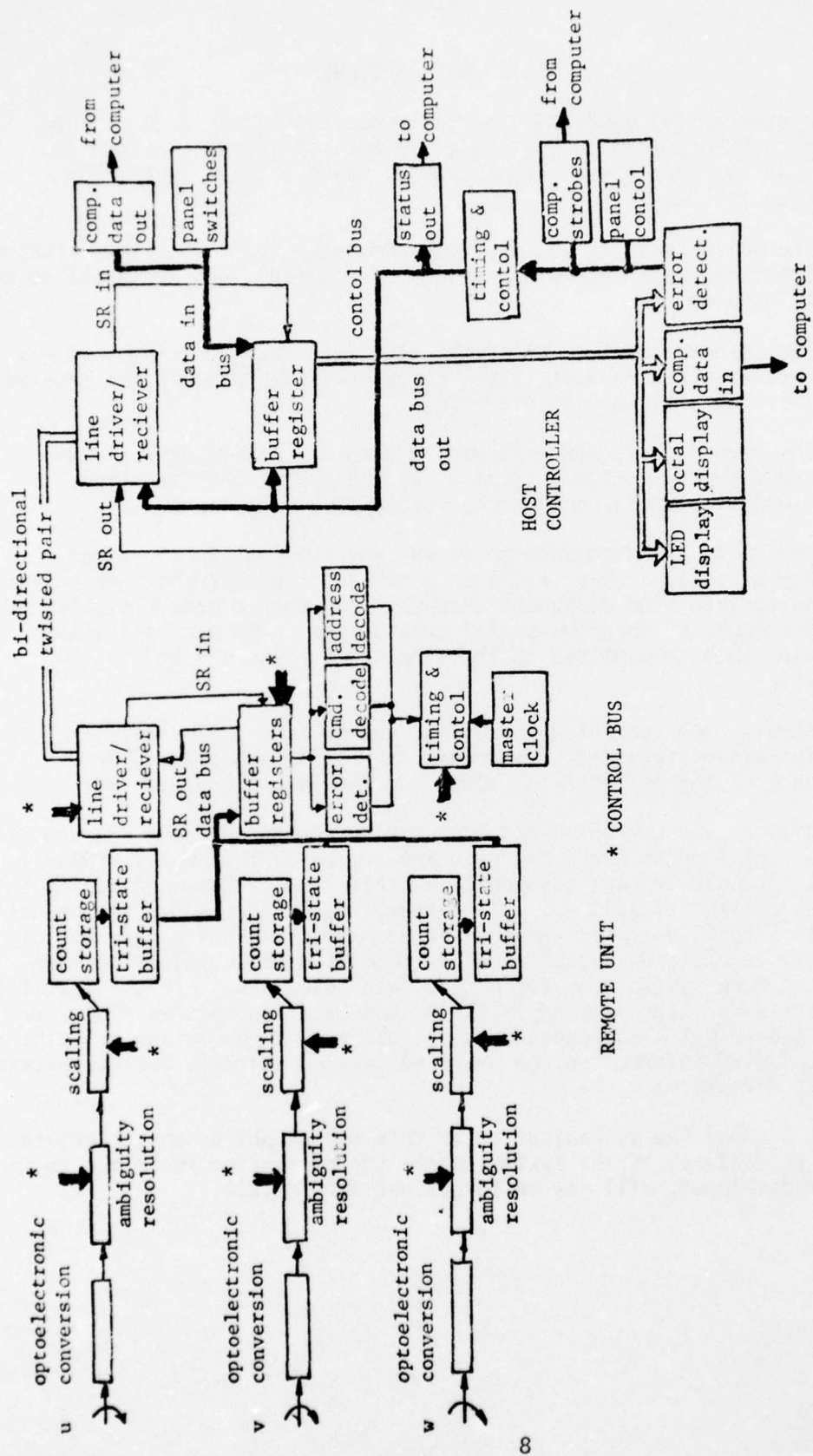


Figure 3. System structure.

Hardware Consideration

Anemometer. Figure 4 shows the developed anemometer (not to scale). The anemometer uses a shaft encoding disk to convert shaft rotations into electronic pulses. The overlapping slots on the disk will create distinctive pulse patterns for clockwise and anticlockwise rotations. The two channels of optically sensed data are presented to the ambiguity resolution circuit (Appendix). The count and sign information created in the ambiguity resolver is sent to the scaling preprocessor.

Scaler. The up/down counter used to accumulate the shaft rotation counts was 16 bits in length in the horizontal U-V directions. Upon computer request, the 16-bit count would be transmitted asynchronously back to the computer. However, under high average wind conditions and long averaging intervals, the up/down counter could easily overflow within an averaging interval. To overcome the problem of inter-interval overflow, a programmed divider, or scaler, was used. The division options are 1, 2, 4, and 16. The user will initially specify a scale factor. During execution, if the data are in danger of causing an overflow within an averaging interval, system software will automatically cause the next largest scale factor to be implemented. Since vertical winds (i.e., W direction) are of low velocity, no scaling hardware was provided for this component.

Timing and Control. The developed system used a 1 MHz CMOS crystal control clock. Sixteen clock pulses were used to define a data bit interval. The resulting 62.5 kHz data rate exceeded an a priori design acquisition rate of 0.5 second per system measurement. The reduced data rate will also allow the system to communicate over lengths in excess of 5 km. If higher data rates were required, a higher master clock rate could be used. However, the increased data rate would result in shorter transmission lengths and increased power requirements (i.e., CMOS power requirements are proportional to speed of operation).

Line Drivers. The line drivers used were National 7831 (see the insert diagram of Fig. 2).

Microprocessor. A National IMP-16-P microprocessor was interfaced to the developed system through the use of tri-state logic. The computer controlled the anemometer system through the issuance of scaling, termination counting, clear counters, and data request commands. Each component of wind at each station was assigned a unique random access address. The address was coded on an 8-pole DIP switch. An ASR-33 teletype was used as a hard copy data logger, program input device, and operator console. The operating system can be entered from paper tape or from four 8 by 256 programmable read only memories (PROMS). Figure 5 is a block diagram of the developed data acquisition software system.

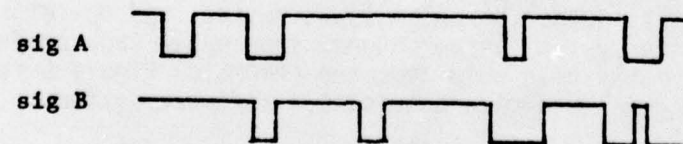
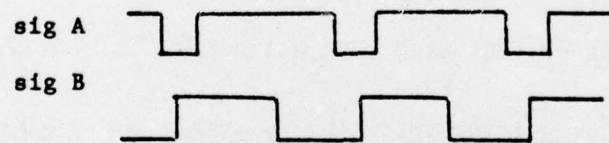
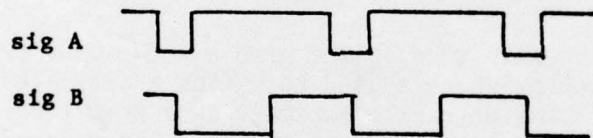
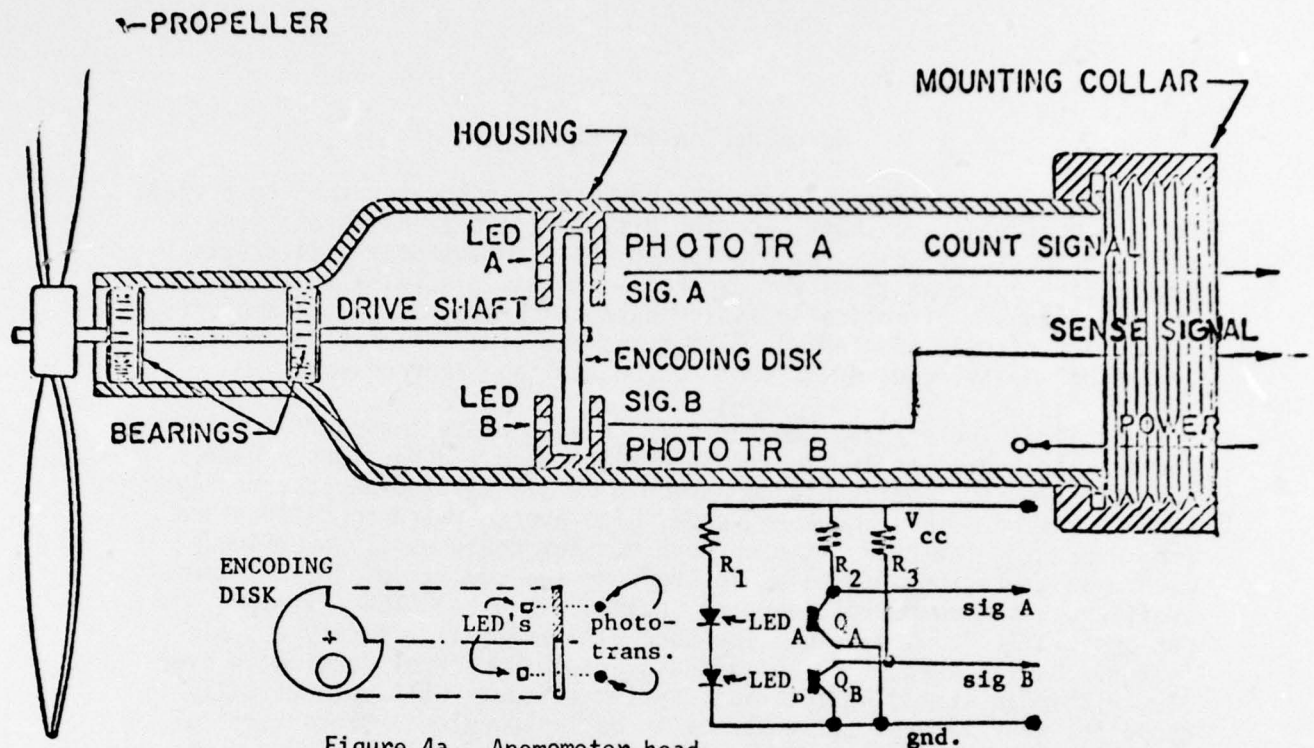


Figure 4. Opto-electronic conversion system.

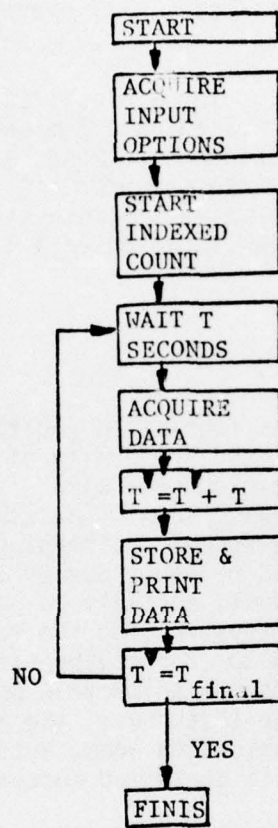


Figure 5. Data Acquisition Program.

OPERATION

Once the system has been field assembled and the operating system loaded, the operator initiates the program. Under the prompting of the computer, the user enters calendar, time of day, averaging interval, total time, and initial scaling information. The system will operate automatically thereafter.

Line fault analysis is performed by issuing a clear, start count, transmit data command to each remote address. Based on a 3 m/sec latency between a start followed immediately by a stop count command, a wind of less than 100 m/sec will return a zero count to the computer. A line fault is indicated by the reception of 17777₈. Since each remote station's position is known on the communication line, the location of a line fault can be easily determined.

RESULTS

A system as described in this work was fabricated and tested at Biggs Army Airfield, El Paso, Texas, and at the University of Texas at El Paso. The remote station was assembled on a wire wrap prototyping board and mounted in a 9 by 9 by 3 chassis box. The computer interface and control was mounted on a 144-socket prototyping I/O card. The system has operated accurately and reliably during the initial test phase. Anemometer calibration would normally be performed in a low-speed wind tunnel. The developed system used the manufacturer's propeller-to-wind speed conversion factor for calibration. The system operated unattended for 30 days with a 6-V motorcycle battery at the prototype remote stations. During the test phase, the ambiguity resolution circuit asynchronous communication loop, automated overflow protection software, and fault analysis performed successfully.

Data samples obtained during the evaluation phase are presented in Figs. 6 through 8. The data are to be interpreted with respect to the following format:

MONTH	DAY	##	##	identify
GMT: HRS	MINS	##	##	experiment
TOT TM: HR	MN	##	##	total time
INTRVL: MN	SC	##	##	averaging interval
DIV INDX		##	###	division index
				0000 = ÷ 1
				0001 = ÷ 2
				0002 = ÷ 4
				0003 = ÷ 16
CALIB: +/-	### - ###			(+ or - nominal value)

Data

Hour Minute S = U Component (M/S) S = V Component (M/V) S = W Component (M/S)

where

$$S = a_1 a_2 a_3 a_4 a_5 = 10a_1 + a_2 + 10^{-1} a_3 + 10^{-2} a_4 + 10^{-3} a_5$$

During the prototype evaluation phase, the U, V, and W channels were driven by a common anemometer. This technique was used because: (1) successful U, V, W operation could be easily verified (i.e., all three channels should present similar data), and (2) it reduced the cost of building a prototype system since only one anemometer needed to be fabricated.

The partial data base presented in Fig. 6 represents the result of a 5-minute experiment using 5-second averaging intervals. Calibration data were supplied from manufacturer's suggestions, and the division index was chosen to be $000 = 1$. The wind value was near 3.6 msec. Figure 7 describes another test performed under similar experimental conditions, except the calibration factor was given a positive correction from its nominal value.

The partial data base shown in Fig. 8 represents an experiment with a simulated high wind derived from a 16-inch fan. In the presence of high winds, a division index of $0003 = 16$ was chosen. The first test (Fig. 8a) was performed with the anemometer in an upwind position for 5 minutes and the data logged (note the algebraically negative winds). The program was reinitiated with the anemometer in a downwind position. All but the first 5-second data record were positive. The first record was negative because the anemometer was reversed during the first 5-second averaging interval of experiment described in Fig. 8b. The absolute magnitudes of the winds (Figs. 8a and 8b) are different because the anemometer was not in perfect orthogonal up and down wind positions. The data presented in Fig. 9 represent a partial record of a 1-hour 30-second averaging interval experiment performed on 11 November 1975 at Biggs Army Airfield, El Paso, Texas. The average windspeed ranged from 7.616 m/sec at 14 hours 4 minutes 30 seconds GMT to 2.145 m/sec at 14 hours 56 minutes 30 seconds GMT. For demonstration, the rotor was manually blocked and rotated counterclockwise during execution. Figure 9 shows results of these actions.

The W component found at 2 minutes 30 seconds into the experiment is seemingly in error. The negative -38921 count is due to an overflow of the 12-bit W accumulator. No W component overflow protection was provided (see item 5 of the system architecture description) since vertical winds were assumed to be of low velocity. The actual wind

MONTH DAY00 25
 GMT:HRS MINS16 30
 TOT TIME:MN 04
 INTRVL:MN SC00 05
 DIV INDX: 0000

CALIB: +/- 000-000

PRESS RUNI

00000	05	03569	03569	03569
00000	10	03505	03441	03505
00000	15	03505	03569	03505
00000	20	03633	03569	03633
00000	25	03569	03633	03569
00000	30	03505	03505	03505
00000	35	03505	03505	03505
00000	40	03569	03569	03569
00000	45	03633	03633	03633
00000	50	03505	03505	03505
00000	55	03633	03633	03633
00001	00	03633	03633	03633
00001	05	03505	03505	03505
00001	10	03633	03569	03633
00001	15	03505	03569	03505

Figure 6. Laboratory experiment.

MONTH DAY00 25
 GMT:HRS MINS16 20
 TOT TIME:MN 08
 INTRVL:MN SC00 10
 DIV INDX: 0000

CALIB: +/- 000+222

PRESS RUNI

00000	10	03826	03826	03826
00000	20	03861	03826	03861
00000	30	03722	03757	03722
00000	40	03861	03861	03861
00000	50	03931	03931	03931
00001	00	03826	03826	03826
00001	10	03826	03826	03826
00001	20	03757	03757	03757
00001	30	03757	03757	03757
00001	40	03757	03757	03757
00001	50	03757	03757	03757
00002	00	03931	03931	03931
00002	10	03826	03826	03826
00002	20	03826	03826	03826
00002	30	03861	03861	03861

Figure 7. Laboratory experiment.

MONTH DAY08 25
 GMT:HP5 MIN520 17
 TOT TH:HP MN00 04
 INTR:LINN SC00 05
 DIV INDX: 0003

CALID: +/-000-000

PRESS RUN1

00000	05	-	38752	-	39771	-	38815
00000	10	-	37732	-	37732	-	37732
00000	15	-	37732	-	37732	-	37668
00000	20	-	36712	-	36712	-	37477
00000	25	-	37732	-	37732	-	37158
00000	30	-	37732	-	37732	-	36967
00000	35	-	36712	-	36712	-	36712
00000	40	-	36712	-	36712	-	37477
00000	45	-	36712	-	36712	-	36393
00000	50	-	36712	-	36712	-	35947
00000	55	-	36712	-	36712	-	36521
00001	00	-	35692	-	35692	-	35628
00001	05	-	36712	-	36712	-	35883
00001	10	-	37732	-	37732	-	37158
00001	15	-	36712	-	36712	-	36839
00001	20	-	36712	-	36712	-	36202
00001	25	-	36712	-	36712	-	36903

MONTH DAY08 25
 GMT:HP5 MIN520 28
 TOT TH:HP MN00 04
 INTR:LINN SC00 05
 DIV INDX: 0003

CALID: +/-000+000

PRESS RUN1

00000	05	-	25728	-	25728	-	45890
00000	10	-	32633	-	32633	-	32951
00000	15	-	32633	-	33653	-	32760
00000	20	-	30593	-	30593	-	30657
00000	25	-	31613	-	31613	-	31677
00000	30	-	31613	-	31613	-	31358
00000	35	-	30593	-	30593	-	30466
00000	40	-	30593	-	30593	-	30529
00000	45	-	30593	-	30593	-	30721
00000	50	-	29573	-	29573	-	29127
00000	55	-	29573	-	29573	-	30020
00001	00	-	30593	-	30593	-	30003
00001	05	-	28554	-	28554	-	29382
00001	10	-	28554	-	28554	-	28617
00001	15	-	29573	-	29573	-	29191
00001	20	-	28554	-	28554	-	29127
00001	25	-	29573	-	29573	-	29000
00001	30	-	28554	-	28554	-	28617

Figure 8. Laboratory experiment.

COPY AVAILABLE TO DDC DOES NOT
 PERMIT FULLY LEGIBLE PRODUCTION

MONTH DAY11 19
 GMT:HPS MINS13 59
 TOT TM:HR MN01 00
 INTFVL:MN SC00 30
 DIV INDX: 0000

CALIB: +/-0000000

PRESS RUN!

00000	30	04674	04674	04674	
00001	00	04865	04865	04865	
00001	30	04716	04716	04716	
00002	00	04886	04886	04897	
00002	30	04599	04589	- 38921 *	
00003	00	05715	05725	05715	
00003	30	03409	03409	03409	
00004	00	00000	00000	00000	} ROTOR ROTATION STOPPED MANUALLY
00004	30	00000	00000	00000	
00005	00	00000	00000	00000	
00005	30	00000	00000	00000	
00005	00	03845	03845	03845	
00006	00	07616	07616	07616	
00006	30	05162	05162	05162	
00007	00	00000	00000	00000	
00007	30	- 00424	- 00435	- 00424	} CLOCKWISE ROTATION CAUSED MANUALLY
00008	00	- 00435	- 00435	- 00435	
00008	30	- 00424	- 00414	- 00424	
00009	00	04079	04079	04079	
00009	30	05226	05226	05226	
00010	00	04737	04727	04737	
00032	00	03802	03802	03802	
00032	30	02379	02379	02379	
00033	00	02676	02676	02687	
00033	30	02443	02443	02443	
00034	00	02591	02591	02591	
00034	30	03293	03293	03293	
00035	00	02953	02953	02942	
00035	30	03441	03420	03441	
00036	00	03909	03930	03919	
00036	30	04886	04886	04875	
00037	00	04206	04206	04206	
00037	30	03335	03335	03335	
00055	30	03399	03399	03399	
00056	00	03633	03633	03633	
00056	30	03378	03378	03367	
00057	00	02273	02273	02273	
00057	30	02145	02145	02145	
00058	00	02698	02698	02708	
00058	30	02889	02889	02889	
00059	00	02825	02825	02825	
00059	30	02698	02698	02687	

END

Figure 9. Field experiment.

MONTH DAY38 25
 GMT:HR5 MIN520 10
 TOT T:HP WNO0 07
 INTPUL:HN SC00 10
 DIV INDX: 0000

CALIB: +/- 000-000

PFESS RUN1

00000 10	03441	03441	03473
00000 20	03569	03569	03537
00000 30	03537	03537	03537
00000 40	03505	03505	03505
00000 50	03537	03537	03537
EPPOR*			
00001 00	- 17623	- 17623	00000
EPPOR*			
00001 10	00000	00000	00000
00001 20	29542	29542	11918
00001 30	03473	03473	03473
00001 40	03525	03525	03505
00001 50	03537	03537	03537
00002 00	03569	03569	03569
00002 10	03601	03569	03601
00002 20	03633	03664	03633
EPPOR*			
00002 30	- 17878	- 17878	00000
EPPOR*			
00002 40	00000	00000	00000
00002 50	29988	29988	12110
00003 00	03569	03569	03569
00003 10	03537	03537	03537
00003 20	03505	03505	03505
00003 30	03473	03473	03473
00003 40	03505	03505	03505
00003 50	03569	03569	03569
00004 00	03473	03473	03473
EPPOR*			
00004 10	- 21096	- 21096	00000
00004 20	28968	28968	07671
00004 30	03569	03569	03569
00004 40	03537	03537	03569
00004 50	03537	03537	03537
00005 00	03505	03505	03505
00005 10	03537	03537	03537
00005 20	03601	03601	03601
00005 30	03441	03441	03441
00005 40	03409	03409	03409
00005 50	03537	03537	03537
00006 00	03505	03505	03505
00006 10	03505	03505	03505
00006 20	03601	03601	03601
00006 30	03505	03505	03505
00006 40	03569	03569	03569
00006 50	03537	03537	03537

END

Figure 10. Error detection.

COPY AVAILABLE TO DDC DOES NOT
 PERMIT FULLY LEGIBLE PRODUCTION

count loaded into the W direction accumulator was obtained from the horizontally deployed anemometer. The high count found in this direction caused the W component to overflow before the U and V component overflow test caused a system clear command to be issued.

Figure 3 dramatizes what would occur if a line fault were detected. During execution, a series of line faults were induced and detected, and the event was logged on the teletype. The system will detect absence of count due to remote station failure, noise corrupting framing code, or communication line failure.

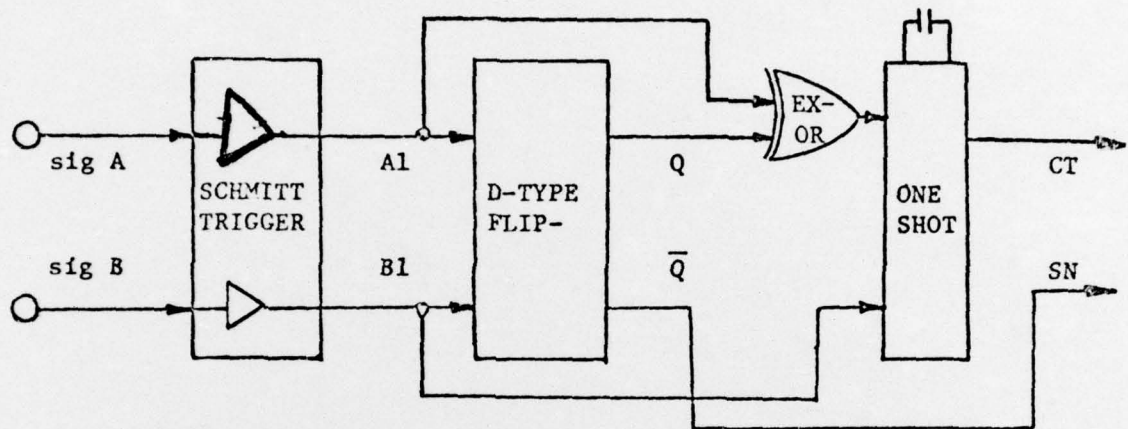
CONCLUSIONS

The developed system satisfies the a priori design criterion. Instrument flexibility was achieved through the use of a microprocessor. The microprocessor capability handled the electronic control and simple data logging responsibilities. It can also serve as a computer and a mass storage device communications controller; therefore, the system can be integrated into a sophisticated meteorological data acquisition system. The system has performed without fault over extended periods of time in both laboratory and field environments. A new feature or modification, the use of a magnetic proximity shaft encoder instead of an LED device, is suggested for inclusion in any production model. This modification and the use of low power MOS line drivers would allow the system to operate at a 25 MW level.

APPENDIX

Ambiguity Resolution Circuit

The ambiguity circuit which inhibits oscillatory shaft fluctuations is described below.



The outputs of the photo-transistors, namely sig. A and sig. B (Fig. 4), are the two inputs to the Schmitt Trigger A (MC14583) which have built-in hysteresis for improved noise immunity. The output A1 is latched into the flip-flop B at the rising edge of A2. The falling edge of A2 is used to trigger the one-shot D (MC14528), which results in a short pulse at the output of the one-shot. However, the output pulse is inhibited if the state of A1 (stored in the flip-flop B) is the same as A1 at the falling edge of A2.

For normal rotation (Fig. 4b or 4c), the one-shot is enabled and a clock pulse results at CT. However, if the anemometer shaft merely oscillates about a point (Fig. 4d), the one-shot is disabled and a no-count results.

The output \bar{Q} of the flip-flop is dependent on the direction of rotation and will be HIGH for one direction and LOW for the other.

REFERENCES

1. Middleton, Meteorological Instruments, John Hopkins Press, Baltimore, Maryland.
2. Peatman, John B., The Design of Digital Systems, McGraw Hill, New York, 1972.

ATMOSPHERIC SCIENCES RESEARCH PAPERS

1. Lindberg, J.D., "An Improvement to a Method for Measuring the Absorption Coefficient of Atmospheric Dust and other Strongly Absorbing Powders," ECOM-5565, July 1975.
2. Avara, Elton, P., "Mesoscale Wind Shears Derived from Thermal Winds," ECOM-5566, July 1975.
3. Gomez, Richard B. and Joseph H. Pierluissi, "Incomplete Gamma Function Approximation for King's Strong-Line Transmittance Model," ECOM-5567, July 1975.
4. Blanco, A.J. and B.F. Engebos, "Ballistic Wind Weighting Functions for Tank Projectiles," ECOM-5568, August 1975.
5. Taylor, Fredrick J., Jack Smith, and Thomas H. Pries, "Crosswind Measurements through Pattern Recognition Techniques," ECOM-5569, July 1975.
6. Walters, D.L., "Crosswind Weighting Functions for Direct-Fire Projectiles," ECOM-5570, August 1975.
7. Duncan, Louis D., "An Improved Algorithm for the Iterated Minimal Information Solution for Remote Sounding of Temperature," ECOM-5571, August 1975.
8. Robbiani, Raymond L., "Tactical Field Demonstration of Mobile Weather Radar Set AN/TPS-41 at Fort Rucker, Alabama," ECOM-5572, August 1975.
9. Miers, B., G. Blackman, D. Langer, and N. Lorimier, "Analysis of SMS/GOES Film Data," ECOM-5573, September 1975.
10. Manquero, Carlos, Louis Duncan, and Rufus Bruce, "An Indication from Satellite Measurements of Atmospheric CO₂ Variability," ECOM-5574, September 1975.
11. Petracca, Carmine and James D. Lindberg, "Installation and Operation of an Atmospheric Particulate Collector," ECOM-5575, September 1975.
12. Avara, Elton P. and George Alexander, "Empirical Investigation of Three Iterative Methods for Inverting the Radiative Transfer Equation," ECOM-5576, October 1975.
13. Alexander, George D., "A Digital Data Acquisition Interface for the SMS Direct Readout Ground Station—Concept and Preliminary Design," ECOM-5577, October 1975.
14. Cantor, Israel, "Enhancement of Point Source Thermal Radiation Under Clouds in a Nonattenuating Medium," ECOM-5578, October 1975.
15. Norton, Colburn and Glenn Hoidale, "The Diurnal Variation of Mixing Height by Month over White Sands Missile Range, NM," ECOM-5579, November 1975.
16. Avara, Elton P., "On the Spectrum Analysis of Binary Data," ECOM-5580, November 1975.
17. Taylor, Fredrick J., Thomas H. Pries, and Chao-Huan Huang, "Optimal Wind Velocity Estimation," ECOM-5581, December 1975.
18. Avara, Elton P., "Some Effects of Autocorrelated and Cross-Correlated Noise on the Analysis of Variance," ECOM-5582, December 1975.
19. Gillespie, Patti S., R.L. Armstrong, and Kenneth O. White, "The Spectral Characteristics and Atmospheric CO₂ Absorption of the Ho⁺:YLF Laser at 2.05 μ m," ECOM-5583, December 1975.
20. Novlan, David J., "An Empirical Method of Forecasting Thunderstorms for the White Sands Missile Range," ECOM-5584, February 1976.
21. Avara, Elton P., "Randomization Effects in Hypothesis Testing with Autocorrelated Noise," ECOM-5585, February 1976.
22. Watkins, Wendell R., "Improvements in Long Path Absorption Cell Measurement," ECOM-5586, March 1976.

23. Thomas, Joe, George D. Alexander, and Marvin Dubbin, "SATTEL — An Army Dedicated Meteorological Telemetry System," ECOM-5587, March 1976.
24. Kennedy, Bruce W. and Delbert Bynum, "Army User Test Program for the RDT&E-XM-75 Meteorological Rocket," ECOM-5588, April 1976.
25. Barnett, Kenneth M., "A Description of the Artillery Meteorological Comparisons at White Sands Missile Range, October 1974 — December 1974 ('PASS' — Prototype Artillery [Meteorological] Subsystem)," ECOM-5589, April 1976.
26. Miller, Walter B., "Preliminary Analysis of Fall-of-Shot From Project 'PASS'," ECOM-5590, April 1976.
27. Avara, Elton P., "Error Analysis of Minimum Information and Smith's Direct Methods for Inverting the Radiative Transfer Equation," ECOM-5591, April 1976.
28. Yee, Young P., James D. Horn, and George Alexander, "Synoptic Thermal Wind Calculations from Radiosonde Observations Over the Southwestern United States," ECOM-5592, May 1976.
29. Duncan, Louis D. and Mary Ann Seagraves, "Applications of Empirical Corrections to NOAA-4 VTPR Observations," ECOM-5593, May 1976.
30. Miers, Bruce T. and Steve Weaver, "Applications of Meteorological Satellite Data to Weather Sensitive Army Operations," ECOM-5594, May 1976.
31. Sharenow, Moses, "Redesign and Improvement of Balloon ML-566," ECOM-5595, June 1976.
32. Hansen, Frank V., "The Depth of the Surface Boundary Layer," ECOM-5596, June 1976.
33. Pinnick, R.G. and E.B. Stenmark, "Response Calculations for a Commercial Light-Scattering Aerosol Counter," ECOM-5597, July 1976.
34. Mason, J. and G.B. Hoidale, "Visibility as an Estimator of Infrared Transmittance," ECOM-5598, July 1976.
35. Bruce, Rufus E., Louis D. Duncan, and Joseph H. Pierluissi, "Experimental Study of the Relationship Between Radiosonde Temperatures and Radiometric-Area Temperatures," ECOM-5599, August 1976.
36. Duncan, Louis D., "Stratospheric Wind Shear Computed from Satellite Thermal Sounder Measurements," ECOM-5800, September 1976.
37. Taylor, F., P. Mohan, P. Joseph and T. Pries, "An All Digital Automated Wind Measurement System," ECOM-5801, September 1976.

DISTRIBUTION LIST

Commanding Officer
Picatinny Arsenal
ATTN: SARPA-TS-S, #59
Dover, NJ 07801

Commanding Officer
Harry Diamond Laboratory
ATTN: Library
2800 Powder Mill Road
Adelphi, MD 20783

Commander
US Army Electronics Command
ATTN: DRSEL-RD-D
Fort Monmouth, NJ 07703

Naval Surface Weapons Center
Code DT 21 (Ms. Greeley)
Dahlgren, VA 22448

Air Force Weapons Laboratory
ATTN: Technical Library (SUL)
Kirtland AFB, NM 87117

Director
US Army Engr Waterways Exper Sta
ATTN: Library Branch
Vicksburg, MS 39180

Commander
US Army Electronics Command
ATTN: DRSEL-CT-D
Fort Monmouth, NJ 07703

Meteorologist in Charge
Kwajalein Missile Range
PO Box 67
APO
San Francisco, CA 96555

Environmental Protection Agency
Meteorology Laboratory
Research Triangle Park, NC 27711

Chief, Technical Services Div
DCS/Aerospace Sciences
ATTN: AWS/DNTI
Scott AFB, IL 62225

Air Force Cambridge Rsch Labs
ATTN: LCH (A. S. Carten, Jr.)
Hanscom AFB
Bedford, MA 01731

Department of the Air Force
16WS/DO
Fort Monroe, VA 23651

Director
US Army Ballistic Research Lab
ATTN: DRXBR-AM
Aberdeen Proving Ground, MD 21005

Geophysics Division
Code 3250
Pacific Missile Test Center
Point Mugu, CA 93042

National Center for Atmos Res
NCAR Library
PO Box 3000
Boulder, CO 80303

William Peterson
Research Association
Utah State University, UNC 48
Logan, UT 84322

Commander
US Army Dugway Proving Ground
ATTN: MT-S
Dugway, UT 84022

Head, Rsch and Development Div (ESA-131)
Meteorological Department
Naval Weapons Engineering Support Act
Washington, DC 20374

Commander
US Army Electronics Command
ATTN: DRCDE-R
5001 Eisenhower Avenue
Alexandria, VA 22304

Marine Corps Dev & Educ Cmd
Development Center
ATTN: Cmd, Control, & Comm Div (C³)
Quantico, VA 22134

Commander
US Army Electronics Command
ATTN: DRSEL-WL-D1
Fort Monmouth, NJ 07703

Commander
US Army Missile Command
ATTN: DRSMI-RFGA, B. W. Fowler
Redstone Arsenal, AL 35809

Dir of Dev & Engr
Defense Systems Div
ATTN: SAREA-DE-DDR
H. Tannenbaum
Edgewood Arsenal, APG, MD 21010

Mr. William A. Main
USDA Forest Service
1407 S. Harrison Road
East Lansing, MI 48823

Naval Surface Weapons Center
Technical Library and Information
Services Division
White Oak, Silver Spring, MD 20910

Dr. A. D. Belmont
Research Division
PO Box 1249
Control Data Corp
Minneapolis, MN 55440

Dir, Elec Tech and Devices Lab
US Army Electronics Command
ATTN: DRSEL-TL-D, Bldg 2700
Fort Monmouth, NJ 07703

Director
Development Center MCDEC
ATTN: Firepower Division
Quantico, VA 22134

Commander
US Army Proving Ground
ATTN: Technical Library, Bldg 2100
Yuma, AZ 85364

US Army Liaison Office
MIT-Lincoln Lab, Library A-082
PO Box 73
Lexington, MA 02173

Library-R-51-Tech Reports
Environmental Research Labs
NOAA
Boulder, CO 80302

Head, Atmospheric Research Section
National Science Foundation
1800 G. Street, NW
Washington, DC 20550

Commander
US Army Missile Command
ATTN: DRSMI-RR
Redstone Arsenal, AL 35809

Commandant
US Army Field Artillery School
ATTN: Met Division
Fort Sill, OK 73503

Meteorology Laboratory
AFCRL/LY
Hanscom AFB
Bedford, MA 01731

Commander
US Army Engineer Topographic Lab
(STINFO CENTER)
Fort Belvoir, VA 22060

Commander
US Army Missile Command
ATTN: DRSMI-RRA, Bldg 7770
Redstone Arsenal, AL 35809

Air Force Avionics Lab
ATTN: AFAL/TSR
Wright-Patterson AFB, Ohio 45433

Commander
US Army Electronics Command
ATTN: DRSEL-VL-D
Fort Monmouth, NJ 07703

Commander
USAICS
ATTN: ATSI-CTD-MS
Fort Huachuca, AZ 85613

E&R Center
Bureau of Reclamation
ATTN: Bldg 67, Code 1210
Denver, CO 80225

HQDA (DAEN-RDM/Dr. De Percin)
Forrestal Bldg
Washington, DC 20314

Commander
Air Force Weapons Laboratory
ATTN: AFWL/WE
Kirtland AFB, NM 87117

Commander
US Army Satellite Comm Agc
ATTN: DRCPM-SC-3
Fort Monmouth, NJ 07703

Commander
US Army Electronics Command
ATTN: DRSEL-MS-TI
Fort Monmouth, NJ 07703

Commander
US Army Electronics Command
ATTN: DRSEL-GG-TD
Fort Monmouth, NJ 07703

Dr. Robert Durrenberger
Dir, The Lab of Climatology
Arizona State University
Tempe, AZ 85281

Commander
Headquarters, Fort Huachuca
ATTN: Tech Ref Div
Fort Huachuca, AZ 85613

Field Artillery Consultants
1112 Becontree Drive
ATTN: COL Buntyn
Lawton, OK 73501

Commander
US Army Nuclear Agency
ATTN: ATCA-NAW
Building 12
Fort Bliss, TX 79916

Director
Atmospheric Physics & Chem Lab
Code 31, NOAA
Department of Commerce
Boulder, CO 80302

Dr. John L. Walsh
Code 5503
Navy Research Lab
Washington, DC 20375

Commander
US Army Air Defense School
ATTN: C&S Dept, MSLSCI Div
Fort Bliss, TX 79916

Director National Security Agency
ATTN: TDL (C513)
Fort George G. Meade, MD 20755

USAF EPAC/CBT (Stop 825)
ATTN: Mr. Burgmann
Scott AFB, IL 62225

Armament Dev & Test Center
ADTC (DLOSL)
Eglin AFB, Florida 32542

Commander
US Army Ballistic Rsch Labs
ATTN: DRXBR-IB
Aberdeen Proving Ground, MD 21005

Director
Naval Research Laboratory
Code 2627
Washington, DC 20375

Commander
Naval Elect Sys Cmd HQ
Code 51014
Washington, DC 20360

The Library of Congress
ATTN: Exchange & Gift Div
Washington, DC 20540
2

CO, US Army Tropic Test Center
ATTN: STETC-MO-A (Tech Lib)
APO New York 09827

Commander
Naval Electronics Lab Center
ATTN: Library
San Diego, CA 92152

Office, Asst Sec Army (R&D)
ATTN: Dep for Science & Tech
Hq, Department of the Army
Washington, DC 20310

Director
US Army Ballistic Research Lab
ATTN: DRXBR-AM, Dr. F. E. Niles
Aberdeen Proving Ground, MD 21005

Commander
Frankford Arsenal
ATTN: Library, K2400, Bldg 51-2
Philadelphia, PA 19137

Director
US Army Ballistic Research Lab
ATTN: DRXBR-XA-LB
Bldg 305
Aberdeen Proving Ground, MD 21005

Dir, US Naval Research Lab
Code 5530
Washington, DC 20375

Commander
Office of Naval Research
Code 460-M
Arlington, VA 22217

Commander
Naval Weather Service Command
Washington Navy Yard
Bldg 200, Code 304
Washington, DC 20374

Technical Processes Br
D823
Room 806, Libraries Div NOAA
8060 13th St
Silver Spring, MD 20910

The Environmental Rsch Institute of MI
ATTN: IRIA Library
PO Box 618
Ann Arbor, MI 48107

Redstone Scientific Info Center
ATTN: Chief, Documents
US Army Missile Command
Redstone Arsenal, AL 35809

Commander
Edgewood Arsenal
ATTN: SAREA-TS-L
Aberdeen Proving Ground, MD 21010

Sylvania Elec Sys Western Div
ATTN: Technical Reports Library
PO Box 205
Mountain View, CA 94040

Commander
US Army Security Agency
ATTN: IARD-OS
Arlington Hall Station
Arlington, VA 22212
2

President
US Army Field Artillery Board
Fort Sill, OK 73503

Commandant
US Army Field Artillery School
ATTN: ATSF-TA-R
Fort Sill, OK 73503

CO, USA Foreign Sci & Tech Center
ATTN: DRXST-ISI
220 7th Street, NE
Charlottesville, VA 22901

Commander, Naval Ship Sys Cmd
Technical Library, Rm 3 S-08
National Center No. 3
Washington, DC 20360

Commandant
US Army Signal School
ATTN: ATSN-CD-MS
Fort Gordon, GA 30905

Rome Air Development Center
ATTN: Documents Library
TILD (Bette Smith)
Griffiss Air Force Base, NY 13441

HQ, ESD/DRI/S-22
Hanscom AFB
MA 01731

Commander
Frankford Arsenal
ATTN: J. Helfrich PDSP 65-1
Philadelphia, PA 19137

Director
Defense Nuclear Agency
ATTN: Tech Library
Washington, DC 20305

Department of the Air Force
5WW/DOX
Langley AFB, VA 23665

Commander
US Army Missile Command
ATTN: DRSMI-RER (Mr. Haraway)
Redstone Arsenal, AL 35809

CPT Hugh Albers, Exec Sec
Interdept Committee on Atmos Sci
Fed Council for Sci & Tech
National Sci Foundation
Washington, DC 20550

US Army Research Office
ATTN: DRXRO-IP
PO Box 12211
Research Triangle Park, NC 27709

Dr. Frank D. Eaton
PO Box 3038
University Station
Laramie, Wyoming 82071

Commander
US Army Training & Doctrine Cmd
ATTN: ATCD-SC
Fort Monroe, VA 23651

Commander
US Army Arctic Test Center
ATTN: STEAC-OP-PL
APO Seattle 98733

Mil Assistant for Environmental Sciences
OAD (E & LS), 3D129
The Pentagon
Washington, DC 20301

Commander
US Army Electronics Command
ATTN: DRSEL-GS-H (Stevenson)
Fort Monmouth, NJ 07703

Commander
Eustis Directorate
US Army Air Mobility R&D Lab
ATTN: Technical Library
Fort Eustis, VA 23604

Commander
USACACDA
ATTN: ATCA-CCC-W
Fort Leavenworth, KS 66027

National Weather Service
National Meteorological Center
World Weather Bldg - 5200 Auth Rd
ATTN: Mr. Quiroz
Washington, DC 20233

Commander
US Army Test & Eval Cmd
ATTN: DRSTE-FA
Aberdeen Proving Ground, MD 21005

Commander
US Army Materiel Command
ATTN: DRCRD-SS (Mr. Andrew)
Alexandria, VA 22304

Air Force Cambridge Rsch Labs
ATTN: LKI
L. G. Hanscom Field
Bedford, MA 01730

Commander
Frankford Arsenal
ATTN: SARFA-FCD-0, Bldg 201-2
Bridge & Tarcony Sts
Philadelphia, PA 19137

Director, Systems R&D Service
Federal Aviation Administration
ATTN: ARD-54
2100 Second Street, SW
Washington, DC 20590

Inge Dirmhirn, Professor
Utah State University, UMC 48
Logan, UT 84322

USAFETAC/CB (Stop 825)
Scott AFB
IL 62225

Chief, Aerospace Environ Div
Code ES41
NASA
Marshall Space Flight Center, AL 35802

Director
USAE Waterways Experiment Station
ATTN: Library
PO Box 631
Vicksburg, MS 39180

Defense Documentation Center
ATTN: DDC-TCA
Cameron Station (BLDG 5)
Alexandria, Virginia 22314
12

Commander
US Army Electronics Command
ATTN: DRSEL-CT-S
Fort Monmouth, NJ 07703

Commander
Holloman Air Force Base
6585 TG/WE
Holloman AFB, NM 88330

Commandant
USAFAS
ATTN: ATSF-CD-MT (Mr. Farmer)
Fort Sill, OK 73503
2

Commandant
USAFAS
ATTN: ATSF-CD-C (Mr. Shelton)
Fort Sill, OK 73503
2

Commander
US Army Electronics Command
ATTN: DRSEL-CT-S (Dr. Swingle)
Fort Monmouth, NJ 07703
3